Distribution Agreement

In presenting this thesis as a partial fulfillment of the requirements for a degree from Emory University, I hereby grant to Emory University and its agents the non-exclusive license to archive, make accessible, and display my thesis in whole or in part in all forms of media, now or hereafter now, including display on the World Wide Web. I understand that I may select some access restrictions as part of the online submission of this thesis. I retain all ownership rights to the copyright of the thesis. I also retain the right to use in future works (such as articles or books) all or part of this thesis.

Sanjana Rao April 12, 2016

Inflammasome-Mediated Interleukin-1β Secretion Drives Neutrophilic Airway Inflammation in Cystic Fibrosis

by

Sanjana Rao

Dr. Rabindra M. Tirouvanziam, Ph.D.
Adviser

Biology

Dr. Rabindra M. Tirouvanziam, Ph.D.
Adviser

Dr. Nicole Gerardo, Ph.D.
Committee Member

Dr. Lou Ann Brown, Ph.D.
Committee Member

2016

Inflammasome-Mediated Interleukin-1β Secretion
Drives Neutrophilic Airway Inflammation in Cystic Fibrosis
by

Sanjana Rao

Rabindra M. Tirouvanziam, Ph.D.
Adviser

An abstract of
a thesis submitted to the Faculty of Emory College of Arts and Sciences
of Emory University in partial fulfillment
of the requirements of the degree of
Bachelor of Sciences with Honors

Biology

2016

Abstract
Inflammasome-Mediated Interleukin-1β Secretion
Drives Neutrophilic Airway Inflammation in Cystic Fibrosis
By Sanjana Rao

Cystic fibrosis (CF) patients experience progressive airway destruction due to opportunistic pathogen colonization and neutrophil-dominated chronic inflammation. In order to investigate the inflammatory response promoting disease progression, we assessed neutrophil inflammasomes and the resulting activation of the IL-1 (interleukin-1) pathway, consisting of pro-inflammatory IL-1β signaling and an endogenous inhibitor, interleukin-1 receptor antagonist (IL-1RA). Specifically, we performed *ex vivo* assays of CF human blood and airway samples with comparison to healthy control (HC) subjects and *in vitro* neutrophil inflammasome stimulations. Further, bioactivity of IL-1β was assessed to identify the potential role of IL-1RA in modulating the IL-1β activatory cascade, and to investigate potential correlations with disease severity. Results show that IL-1β production is significantly elevated in CF, compared to HC and chronic obstructive pulmonary disease (COPD) controls, confirming that CF disease is linked with IL-1 signaling. Furthermore, we observed a strong correlation between neutrophil numbers and IL-1β levels, consistent with a pro-inflammatory loop of neutrophil recruitment and IL-1β secretion that itself recruits more neutrophils. Results from inflammasome stimulation and follow-up *in vitro* assays together demonstrate that IL-1β secretion may not be concomitant with cell death, contrary to conventional belief. Finally, using a cell line genetically engineered to detect bioactive IL-1β, we found that IL-1β in CF airway samples is indeed bioactive and that this bioactivity is closely regulated by IL-1RA. Ultimately, results gathered strongly suggest that IL-1β is a clinically relevant modulator of CF, and a potential target for therapeutic intervention.

Inflammasome-Mediated Interleukin-1β Secretion Drives Neutrophilic Airway Inflammation in Cystic Fibrosis

By

Sanjana Rao

Rabindra M. Tirouvanziam, Ph.D.
Adviser

A thesis submitted to the Faculty of Emory College of Arts and Sciences
of Emory University in partial fulfillment
of the requirements of the degree of
Bachelor of Sciences with Honors

Biology

2016

Acknowledgements

I would like to extend my sincerest gratitude to my adviser, Dr. Rabin Tirouvanziam, for giving me the opportunity to work in his laboratory, for constantly challenging me to become a better scientist, and ultimately, for providing me with one of the most invaluable experiences of my undergraduate career at Emory. I would like to acknowledge the entire Tirouvanziam lab for their consistent encouragement and constructive feedback, particularly Osric Forrest for his close, insightful mentorship over four semesters. I would like to thank Dr. Milton Brown for his infinite knowledge, meaningful guidance, and unparalleled patience throughout my project.

Additionally, I would like to thank my honors committee members, Dr. Lou Ann Brown and Dr. Nicole Gerardo, for their generous support, advice, and invested time in the thesis-writing process.

I would also like to thank Emory University and the Biology Department for valuing independent undergraduate research the way they do through both Biology 499 and the Honors Biology 495 courses.

Finally, I would like to thank the Emory Children's Center for providing me with the resources for my experiments. This work was supported by the Emory Children's Center for CF Research Startup Fund and Cystic Fibrosis Foundation (TIROUV15A0) to Dr. Tirouvanziam.

Table of Contents

List of Abbreviations

ABC, ATP-binding cassette
ASC, Apoptosis-associated Speck-like protein
ASL, Airway surface liquid
ASN, Airway supernatant
ATP, Adenosine triphosphate
CF, Cystic Fibrosis
CFTR, Cystic Fibrosis Transmembrane Conductance Regulator
COPD, Chronic obstructive pulmonary disease
ELISA, Enzyme-linked immunosorbent assay
FACS, Fluorescence-activated cell sorting
HC, Healthy control
IL-18, Interleukin-18
IL-1R, Interleukin-1 receptor
IL-1RA, Interleukin-1 receptor antagonist
IL-1β, Interleukin-1β
LDH, Lactate dehydrogenase
LPS, Lipopolysaccharide
MSU, Monosodium urate
NF-κB, Nuclear factor-κB
NLRC4, NLR Family CARD domain-containing protein 4
NLRP3, NLR Family pyrin domain-containing 3
O.D., Optical density
PMA, Phorbol 12-myristate acetate
PMN, Polymorphonuclear neutrophils
SEAP, Secreted embryonic alkaline phosphatase
TLR4, Toll-like receptor 4
TNF-α, Tumor necrosis factor α

I. Introduction

Background: Chronic airway disease due to combined effects of bacterial infection, neutrophil-mediated inflammation, and airway obstruction by inspissated mucus is the primary cause of morbidity and mortality in cystic fibrosis (CF) patients[1]. Currently, approximately 70,000 individuals live with CF worldwide and 1,000 new CF cases are diagnosed each year in the USA[2]. According to the US CF Foundation Patient Registry, between 2000 and 2010, the number of patients suffering from this debilitating disease increased from 21,000 to 26,000 while the median survival age of children born and diagnosed with CF is continuing to increase past 50 years[3]. This significant statistic of greater diagnoses coupled with longer life expectancy has substantial prognostic implications and thus mandates findings amenable to therapeutic intervention in CF patients at all ages.

Genetic basis of CF: CF is an autosomal recessive disorder characterized by a defective gene encoding the cystic fibrosis transmembrane regulator (CFTR) on chromosome 7[4]. The CFTR ion channel is unique among the ATP-binding cassette (ABC) family of transporters, in that it functions as a channel, enabling chloride and bicarbonate ions to be effluxed from the cytosol into the lumen along the preexisting gradient. Consequently, CFTR function is critical for maintenance of salt/water and pH balance of the fluids lining the epithelial surfaces of the lung, digestive system, genital tract, salivary glands, and sweat glands[5]. The most common *cftr* mutation (approximately 70% of alleles) is ΔF508, resulting in the deletion of phenylalanine (F) at position 508 of the CFTR protein. The ΔF508 mutation leads to abnormal folding, defective membrane insertion and conductance[6].

Pathophysiology of CF airway disease: Defective CFTR function caused by the ΔF508 and other mutations is believed to lead to abnormal airway surface liquid (ASL) properties, although it is as yet debated whether abnormal viscosity, pH, or other properties start the pathological process in CF airways. This pathological process is best described as a triad of obstruction, bacterial infection, and inflammation[7,8,9]. Toxic effectors from host inflammatory cells and bacteria damage matrix components of the airways, eventually causing bronchiectasis[10]. CF adversely affects other organs as well, associating notably with chronic sinusitis, abnormal digestive function, pancreatic insufficiency and osteoporosis, among other symptoms[8].

PMN-mediated inflammation in CF: The dominant feature of CF airway inflammation is the massive recruitment of polymorphonuclear neutrophils (PMN) from blood. PMNs are terminally differentiated myeloid cells that comprise 50 – 70% of circulating white blood cells and generally form the first bodily defense against infection[11]. PMNs are a type of granulocytes, characterized by the presence of cytoplasmic granules holding proteolytic and oxidative enzymes that contribute to their bacteria-killing abilities[12]. Paradoxically, the recruitment of blood PMNs into CF lungs coincides with the failure to clear bacteria, including *Staphylococcus aureus* and *Pseudomonas aeruginosa.* Instead PMN-dominated inflammation continues relentlessly, leading to proteolytic destruction of the airway tissue, and ultimately respiratory failure[10]. The conventional wisdom used to be that PMNs were mere bystanders in CF, unable of doing their usual job of destroying bacteria and rapidly dying in the airways. However, recent fluorescence-activated cell sorting (FACS) analyses by the Tirouvanziam group have disproved this conventional paradigm and shown that PMNs remain largely alive after recruitment to the

CF airway lumen. Rather than dying rapidly, PMNs appear to be functionally and metabolically reprogrammed, and their dysfunction is central to both the onset and progression of CF disease.

Inflammasome activation: CF inflammation is thought to be potentiated, in part, by overactive inflammasomes, intracellular multi-protein complexes that regulate the production and secretion of pro-inflammatory cytokines in response to both endogenous and exogenous danger signals[13]. While five major dominant inflammasome complexes have been identified so far, NLR Family, Pyrin Domain Containing 3 (NLRP3) and NLR family CARD domain-containing protein 4 (NLRC4) are the two complexes most conventionally associated with PMN-driven airway inflammation. In particular, studies on NLRP3 have shown that upon activation, this complex undergoes oligomerization and assembly of the apoptosis-associated Speck-like protein (ASC), which comprises a caspase-recruitment domain[14]. Once aggregated, auto-catalytically activated caspase-1, a cysteine-aspartic acid protease, cleaves pro-interleukin-1β (IL-1β) to enable the release of the biologically active form of the molecule[15]. Another member of the IL-1 superfamily, IL-18, is thought to be produced and secreted in a similar fashion, thereby playing a substantial role in promoting inflammation[16,17]. Indeed, a prior study focusing on immunohistochemical analysis showed markedly higher expression of IL-18 in CF patients compared to normal controls[18].

The prevalent model accounting for NLRP3 inflammasome activation in PMNs begins typically with lipopolysaccharide (LPS), a major component of the outer membrane in gram negative bacteria, leading to the transcriptional induction of IL-1β mRNA and subsequent translation into pro-IL-1β via activation of the Toll-like receptor 4

(TLR4) cascade and its downstream transcription factor nuclear factor-κB (NF-κB)[19]. NF-κB binds specific promoter sequences on DNA to modulate the expression of genes encoding cytokines, chemokines, and adhesion molecules involved in inflammatory responses[20]. Coupled with LPS activation, a secondary stimulus is necessary to induce assembly of the NLRP3 inflammasome, inducing caspase-1 activation and subsequent IL-1β production. Interestingly, unlike macrophages, PMNs do not seem to undergo obligatory programmed death by pyroptosis upon inflammasome activation, which may allow them to sustain IL-1β production and thus maximize host antimicrobial defense upon pathogen challenge[21].

***Modulation of the IL-1β pathway*:** A hallmark of chronic PMN-driven inflammation is an increased extracellular level of IL-1β, giving rise to several downstream pro-inflammatory effects and promoting feed-forward recruitment of PMNs[22]. Notably, IL-1β induces its own expression via NF-κB, amplifying the IL-1β response in autocrine and paracrine manner. Several prior studies have highlighted the link between IL-1β presence in the airway fluid (e.g, sputum) and excessive NLRP3 inflammasome activation, as well as its correlation with disease severity, suggesting that this pathway plays a key role in driving the inflammatory response not only in CF, but also in other similar PMN-driven inflammatory diseases[13,23]. Further, studies have shown that neutralization of the IL-1β pathway results in a dramatic reduction of inflammation, thereby making it a prime target for therapy[24,25]. Binding of IL-1β to the ubiquitously expressed IL-1 receptor (IL-1R) induces a conformational change to the receptor, leading to downstream activation of intermediate complexes and transcription factors, including NF-κB[22]. IL-1 receptor antagonist (IL-1RA), a naturally occurring ligand, also binds IL-

1R, but unlike IL-1β, blocks downstream effects altogether[22]. Although IL-1β-dependent inflammation has been studied in PMNs, the suppressive role of IL-1RA on IL-1 signaling in CF has yet to be fully elucidated.

Study rationale: To better delineate the mechanisms underlying PMN-dominated airway inflammation, *ex vivo* assays of CF blood and airway samples and *in vitro* inflammasome stimulations of PMNs were performed. Bioactivity of IL-1β was assessed to identify the potential role of IL-1RA in modulating the IL-1β activatory cascade, and to investigate potential correlations with disease severity. Further, to elucidate the mechanism by which PMNs secrete IL-1β, the correlation between IL-1β production and PMN cytotoxicity was studied. Overall, the contribution of PMNs to bioactive IL-1β in CF airway disease was investigated to substantiate the development of PMN-targeted therapies for CF.

II. Materials and Methods

***Human subjects*:** Samples were obtained through a study approved by the Institutional Review Board at Emory University. All subjects provided written consent prior to participation. HC subjects were >18 years of age and did not include pregnant and breast-feeding women. CF was diagnosed using a quantitative iontophoresis test (sweat chloride: 60mEq/l) and/or proof of two *cftr* mutations. Samples were collected at initial enrollment during hospitalization due to acute pulmonary exacerbation (Visit 1, inpatient), and 3 months (Visit 7, outpatient) and 1 year (Visit 9, outpatient) following enrollment. Inpatient samples were collected 2-5 d after initial oral or intravenous antibiotic treatment and outpatient samples were collected at routine clinical check-ups. CF clinical data included age, gender, mutations, lung function, medications, and microbiology (**Table 1**).

Sample collection and processing: Airway sputum samples were obtained from CF patients by spontaneous expectoration and from HC subjects by induction with hypertonic saline. Sputum was mechanically dissociated using an 18G passage needle after addition of 6 mL PBS with 2.5 mM EDTA and then weighed. Blood was collected by venipuncture from CF and HC subjects. Blood and dissociated sputum were centrifuged and processed to generate platelet-free plasma and cell/bacteria-free airway supernatant (ASN) for pro-inflammatory cytokine quantification and enzymatic activity assays (**Figure 1**). Disease control sputum samples from patients with chronic obstructive pulmonary disease (COPD) were also collected and processed in the same manner.

ELISA: IL-1β was quantified using a human IL-1β Duoset enzyme-linked immunosorbent assay (ELISA) kit (R&D Systems, Minneapolis, MN). The capture antibody (480 µg/mL of mouse anti-human IL-1β) was diluted to 4.0 µg/mL in PBS and was used to coat a 96-well microplate. After a series of three washes with wash buffer (0.05% Tween20 in PBS (PBS-T)), the plate was blocked with reagent diluent [1% bovine serum albumin (BSA) in PBS] and incubated overnight. ASN samples were thawed and diluted in reagent diluent appropriately, and were each added to wells in duplicate. A standard curve was also generated by conducting 2-fold serial dilutions in reagent diluent of a standard solution provided by the kit, beginning at 250 pg/mL. Following a 2-hour incubation at room temperature and three sets of washes with PBS-T, the detection antibody (12 µg/mL of biotinylated goat anti-human IL-1β) was diluted to 200 ng/mL in reagent diluent and added to each well and incubated for l hour at room temperature. After washing the plate four times with PBS-T, a solution of streptavidin conjugated to horseradish-peroxidase (streptavidin-HRP) was diluted to 200 µg/mL and added to each

well. A 20-minute incubation in the dark followed after which substrate solution (1:1 mixture of H_2O_2 and tetramethylbenzidine) was added to each well for approximately 12 minutes while color change occurred, from clear to blue. 2N H_2SO_4 was immediately added as a stop solution, changing the blue color to yellow, and the optical density of each well was subsequently detected using a microplate reader set to 450 nm. IL-1β levels were determined from the standard curve using a 4 parameter, non-linear curve fit.

IL-1RA was quantified using a human IL-1RA Duoset ELISA kit (R&D Systems™, Minneapolis, MN). ELISA protocol was executed as described above for IL-1β, with a standard curve serial dilution beginning at 2500 pg/mL.

IL-18 was quantified using a human IL-18 ELISA kit (RayBiotech, Norcross, GA). A 96-well microplate was pre-coated with antibody specific for human IL-18. Standards and plasma samples were diluted in assay diluent A (diluent buffer + 0.09% sodium azide as preservative) and were each added in duplicate for a 2.5 hour incubation at room temperature with gentle shaking. The solution was discarded and washed 4x with wash buffer (1:20 wash buffer concentrate in deionized water). Biotinylated anti-human IL-18 antibody was diluted 80-fold with assay diluent B and added to each well for a 1-hour incubation at room temperature. After 4 washes, a prepared streptavidin-HRP solution (concentrate diluted 300-fold with assay diluent B) was added to each well for a 45-minute incubation at room temperature. TMB one-step substrate reagent (tetramethylbenzidine in buffer solution) was added to each well for a 30-minute incubation in the dark. Stop solution (0.2M H_2SO_4) was then added to each well, changing the color from blue to yellow, and the intensity of the color was immediately detected using a microplate reader at 450 nm **(Figure 2)**.

Sample normalization: Cytokine concentrations obtained from the spectrophotometer readings were normalized to respective sputum weight (in g) using the following equation: (Cytokine concentration x dilution factor) x ((6 g of PBS with 2.5 mM EDTA + sputum weight)/sputum weight). IL-18 concentrations in CF and HC plasma were not normalized.

Human Embryonic Kidney (HEK)-Blue assay:

Cell growth and maintenance: HEK-Blue-IL-1β cells were purchased from InvivoGen (San Diego, CA). These cells have been engineered to release secreted embryonic alkaline phosphatase (SEAP) if their surface-expressed IL-1 receptors are ligated by IL-1β present in the extracellular fluid **(Figure 3)**. Thus, these cells can be used to test IL-1β bioactivity in fluid samples (e.g., patient airway fluid) in which IL-1β and IL-1RA are present, and the latter is theoretically able to block signaling by the former. HEK-Blue-IL-1β cells were grown at 37ºC with 5% CO_2 in sterile Dulbecco's Modified Eagle Medium with 4500 mg/L glucose, 110 mg/L sodium pyruvate, 2 mM L-Glutamine, 10% heat-inactivated fetal bovine serum, 50 U/mL penicillin, 50 µg/mL streptomycin, and 100 µg/mL normocin, a formulation of three antibiotics active against mycoplasmas, bacteria, and fungi[26]. Growth medium was renewed every other day and cells were passaged upon reaching 75% confluency. After 1.5 weeks, selective media, consisting of sterile growth media, 100 µg/mL zeocin, and 200 µg/mL hygromycin B Gold, was added to the cell culture to maintain IL-1β specificity of the cell line (HEK-Blue-IL-1β cells are resistant to zeocin and hygromycin B). Cells were maintained in selective media at 37ºC with 5% CO_2 for approximately 1 week.

Detection of bioactive IL-1β by HEK-Blue IL-1β cells: Once confluent, cells were mechanically detached from the flask using PBS without Ca^{2+} and Mg^{2+} and pelleted into a conical tube for counting. 10 µL of cell suspension was mixed with 40 µL of acridine orange /

ethidium bromide solution and cell count and viability were assessed via using a hemocytometer. The resuspension volume of selective media was adjusted to yield a concentration of 330,000 cells/mL. 150 µL of cell suspension (50K cells) was added to each well of a 96-well microplate. Human recombinant IL-1β was serially diluted 10-fold in sterile selective media to create 6 standards of positive control: 100, 10, 1, 0.1, 0.01, 0.001 (in ng/mL). As a negative control, human recombinant tumor necrosis factor-α (TNF-α) was serially diluted in the same concentrations, since the HEK-Blue IL-1β cells derive from HEK-Blue TNF-α/IL-1β cells in which the TNF-α response has been blocked. CF and HC ASN samples were diluted 1:15, 1:25, and 1:50 in sterile selective media. 50 µl of standards and samples were added to the cell suspension in each well, all in triplicates (**Figure 4**). (Note: the 1:60, 1:100, and 1:200 final dilutions are indicative of a 4-fold dilution of 1:15, 1:25, and 1:50 sample dilutions, respectively, in cell suspension). The plate was then incubated overnight at 37ºC with 5% CO_2. The following day, Quanti-Blue powder (Invivogen) was reconstituted in warmed endotoxin-free water and filtered on a 0.2um membrane, thus generating a SEAP detection medium. 150 µL of the Quanti-Blue solution was added to each well of a new 96-well microplate. The 96-well microplate with HEK-Blue-IL-1β was then centrifuged at 400G at 4ºC for 10 minutes and 50 µL of supernatant from each well was added to the Quanti-Blue solution in the new microplate and incubated at 37ºC with 5% CO_2. After 45 minutes, the plate was read at 655 nm on a spectrophotometer.

Choice of optimal conditions for HEK-Blue experiments: The final 1:60, 1:100, and 1:200 dilutions were chosen to optimize the dynamic signal range of the assay readouts. In previous experimental replicates, 1:2, 1:10, and 1:100 dilutions were used, however SEAP detection was severely compromised. It was hypothesized that ASN samples were too concentrated in these dilutions, to an extent that SEAP-producing cells were dying and consequently, diminishing the

O.D. signal. Further, within the suggested time frame for Quanti-Blue incubation with induced cell supernatant of 30 minutes – 3 hours, the optimal plate reading point was determined to be 45 minutes. Following 45 minutes, SEAP signal dropped significantly, likely due to degradation of the protein.

In vitro inflammasome activation: Venous blood was drawn from healthy donors in 4-6 10 mL sterile vacutainer blood collection tubes containing potassium EDTA. 5 mL of blood was slowly layered onto 5 mL of Polymorphprep (Nycomed, Zürich, Switzerland) [density: 1.113±0.001g; active ingredients: sodium diatrizoate (13.8% w/v) and dextran 500 (8.0% w/v)], in sterile plastic tubes. Blood was spun for 45 minutes at 350G at 20ºC to create a density gradient (**Figure 5**). Using a sterile suction dropper, the PMN containing layer was transferred to a sterile 50 mL tube and sterile 0.45% NaCl was added to PMNs in 1:1 ratio to restore osmolarity. PMNs were centrifuged for 10 minutes at 350G at 20ºC and the supernatant was decanted. To lyse remaining contaminating erythrocytes, 12 mL of sterile ice cold water was added and gently mixed with cell pellet and within 30 seconds, 12 mL of ice-cold sterile 1.8% NaCl solution was added. After a 5-minute spin at 350 G at 4ºC, the lysis step was repeated (until pellet was visibly white). After decanting the supernatant, isolated PMNs were resuspended in 4 mL sterile ice-cold RPMI 1640 (Corning®, Manassas, VA) and counted on a hemocytometer using the same protocol as described above. Resuspension volume was adjusted to yield 1 x 10^6 PMNs per 25 µl. Equal volumes of purified PMNs (4-8 million cells, depending on donor volume) were added to sterile FACS tubes. Known inflammasome activators such as monosodium urate crystals (MSU, at 250, 50 and 10 µg/ml), LPS (10 ng/mL), adenosine triphosphate (ATP, at 5 mM), and phorbol 12-myristate acetate (PMA, at 20 nM) were diluted in sterile RPMI 1640 to working concentrations and added to respective tubes containing PMNs.

Tubes were incubated at 37ºC with 5% CO_2 for 2 hours with ATP added to the LPS tube for 30 minutes after the 2-hour mark. Whole blood and unstimulated PMNs were incubated on ice for 2 hours as controls. After centrifugation of FACS tubes at 800G for 10 minutes at 4ºC, stimulated supernatants were collected and stored at -80ºC for further assay use. Pelleted PMNs from each condition were washed twice with 3 mL of PBS with 2.5 mM EDTA and processed for flow cytometry analysis, as detailed before[27].

Lactate Dehydrogenase Assay (LDH): A LDH cytotoxicity assay kit (Thermo Fisher Scientific) was used to quantitatively measure extracellular LDH, a cytosolic enzyme released upon cell death, in culture media. LDH quantified by a coupled enzymatic reaction in which a red formazan product is created (**Figure 6**) and measured spectrophotometrically at 490nm. The substrate mix was dissolved in ultrapure water and mixed in the dark with assay buffer to create the reaction mix. 1x LDH positive control was diluted with 1% BSA in PBS to a 1:10,000 ratio. Cell-free supernatants from the above-described stimulation assay and from heat-killed and saponin-lysed PMNs and 50 µL of 1x LDH positive control and sterile RPMI (negative control) were added to 96-well flat-bottom plate in triplicate. 50 µL of reaction mix was transferred to each sample well and mixed thoroughly using a multichannel pipette. The plate was incubated at room temperature for 30 minutes in the dark. 50 µL of stop solution was added to each well and gently mixed. Any persisting air bubbles were broken with syringe needles prior to spectrophotometer reading. Absorbance was measured at 490 nm and 680 nm. LDH activity [$OD_{490\,nm} - OD_{680\,nm}$] was reported as % optical density of the 1xLDH Positive Control.

Heat-killed and saponin-lysed PMNs: To incorporate strong positive controls of death into the LDH cytotoxicity assay, PMNs were heat-killed and lysed with saponin. Purified

PMNs were added to two FACS tube in equal volumes as the other conditions in the inflammasome activation assay. One tube was placed on a metal heating block for 5 minutes and the other was treated with 1mL of Perm/Wash buffer™ (BD Biosciences, San Jose, CA) diluted 1:10 in deionized water for 30 minutes.

***Statistical Analysis**:* Statistical analyses were done using the JMP 10 software (SAS Institute, Cary, NC) and Prism 6 software (GraphPad, La Jolla, CA). Significance of results was determined using the nonparametric Mann-Whitney *U* test with a $p < 0.05$ for box plots and the Spearman's test with a high correlation coefficient (ρ) for correlations.

III. Results

IL-1β and PMN count are significantly up-regulated in CF ASN compared with HC ASN. We hypothesized that CF being a highly inflammation-driven disease, CF airway samples would contain significantly greater amounts of pro-inflammatory markers than samples from HC subjects. ELISA data confirmed that IL-1β concentrations in CF sputum (at all visits) were significantly higher than in HC sputum (**Figure 7a**), as was PMN count (**Figure 7d**). IL-1RA concentrations, however, did not significantly differ across HC and CF samples, but data revealed drastically greater amounts of IL-1RA than IL-1β; this particularly held true for the HC subjects (**Figure 7b,c**).

IL-1β and PMN count are significantly lower during CF inpatient visits compared with CF outpatient visits. Matched pairs analysis also revealed that IL-1RA did not significantly vary across HC and CF samples (**Figure 8a**). IL-1β is significantly correlated with PMN count in CF samples from visits 1 and 7, but not in visit 9 (**Figure 9**).

IL-18 is significantly up-regulated in CF Visit 1 plasma compared to HC plasma, but the same does not hold true for other visits. IL-18 presence was quantified as another caspase-1-produced biomarker, however it was undetectable in both CF and HC ASN. Despite its absence in ASN, IL-18 levels were higher in CF patients at visit 1 than in HC subjects **(Figure 10a)**. There was no significant correlation established between IL-18 concentration in CF plasma and IL-1β concentration in CF ASN **(Figure 10b)**.

Bioactive IL-1β signaling is significantly up-regulated in HEK-Blue IL-1β cells when induced with CF-ASN compared to with HC-ASN. Bioactive IL-1β was calculated as a relative concentration, reflective of SEAP quantity in the supernatant of sensor cells (**Figure 11a)**. Ratios of IL-1β in the supernatant to IL-1RA in the inducing sample did not differ between HC and CF **(Figure 11b)**. There was a strong correlation between the *in vivo* IL-1β concentration of a sample and the detected IL-1β concentration secreted by the cells it induced **(Figure 11c)**.

IL-1β production and secretion is up-regulated in stimulated PMNs compared with unstimulated PMNs. To further elucidate the relationship between inflammasome activation and IL-1β secretion, supernatants of both stimulated and unstimulated PMNs were analyzed for cytokine presence via ELISA. Data showed that PMNs incubated in solely RPMI for 2h versus with a 250μg/mL solution of MSU secreted significantly less IL-1β, as expected **(Figure 12a)**. IL-1β was undetectable upon incubation with 20 nM PMA. Results from the LDH cytotoxicity assay revealed that PMN death was not induced dose-dependently upon MSU stimulation **(Figure 12b)**. ELISA and LDH data for the LPS (10ng/mL) + ATP (5mM) stimulation condition were consistent with the notion that IL-1β secretion is closely linked with cell death, as the supernatant contained highest IL-1β concentration *and* comprised the highest cell death levels (higher than the kit-provided LDH + control, noted by >100%) of the activating ligands.

IL-1β is significantly elevated in CF Visit 7 ASN, compared to HC and COPD patient samples. COPD samples were assayed via ELISA to determine the relationship between pro-inflammatory biomarker profiles of phenotypically similar diseases. Only Visit 7 CF ASN was used here in efforts to avoid duplicate data from the same patients; visit 7 samples were selected over visit 1 ASN since COPD samples are not obtained during exacerbated respiratory episodes, but rather during outpatient follow-ups. Data showed a significantly greater IL-1β concentration in CF patients versus COPD patients and HC subjects, and the latter two had comparable values (**Figure 13**).

IV. Discussion and Future Directions

It is thought that IL-1β plays a significant role in regulating inflammatory responses in CF. The finding that the pro-inflammatory cytokine is significantly up-regulated in CF ASN compared to that of HC subjects is consistent with this notion. Paired analysis showing a significant reduction in IL-1β production *and* PMN count in inpatient vs. outpatient samples suggests that the high-impact therapy patients receive upon hospitalization may interfere with IL-1β signaling, thereby emphasizing its relevance for pharmaceutical intervention. COPD, a chronic lung disease in which airflow is blocked and respiratory function is challenged, share pathophysiological features with CF[28,29,30]. In this study, COPD airway samples contained significantly less IL-1β than CF Visit 7 airway samples, suggesting that despite gross similarities in their PMN-driven inflammatory process, CF and COPD may differ in the intensity of IL-1 signaling. Future *ex vivo* studies of patients with severe asthma would serve as an interesting additional disease comparison.

The high IL-1RA:IL1β ratio measured in airway samples suggested that despite its significant presence, Il-1β may not be bioactive in these samples. Thus, we set out to assess bioactivity of IL-1β in airway samples using the HEK-Blue IL-1β cell model. Our data support the notion that CF ASN-induced cells have greater bioactive IL-1β (higher SEAP signal) in their supernatants compared to those that are induced by HC ASN. Additionally, cells induced by ASN with high IL-1β content yielded high SEAP signal, and conversely. Finally, when CF or HC ASNs with a high IL-1RA:IL-1β ratio were incubated with the cells, the SEAP signal was lower than that measured with cells induced samples with ASN featuring low IL-1RA:IL-1β ratio. Taken together, these results suggest that IL-1β in ASN is bioactive and indeed modulated by IL-1RA. Future experimental replicates with additional CF and HC ASN samples including a co-incubation with a monoclonal anti-IL-1β antibody are needed to ensure a detectable response is blocked so readouts are solely attributable to IL-1β bioactivity.

The strong correlation between PMN count in the lung sputum and IL-1β concentration is consistent with the hypothesis of a pro-inflammatory loop operating in CF. According to this rationale, CF airway PMNs secrete IL-1β leading to sustained IL-1 receptor activation, and in turn, to further blood PMN recruitment to CF airways.[28] Interestingly, IL-18, another pro-inflammatory, caspase 1-dependent, mediator was significantly different in the plasma of CF inpatients compared to HC subjects, although no difference was observed in other visits. This is consistent with inpatient samples being collected during an exacerbation while outpatient samples were collected during stable follow-up visits. IL-18 was undetectable in the ASN, perhaps due to the fact that this

cytokine is vulnerable to proteolytic degradation by neutrophil elastase, a major mediator in CF airway inflammation[31].

In vitro inflammasome stimulations were performed to investigate the possibility of inducing IL-1β production in the supernatants of blood PMNs. To effectively activate the inflammasome, both pathogen- and damage-associated molecular pattern activators were utilized, LPS serving as the former and ATP and MSU as the latter. Inflammasome assembly, activation, and subsequent unfolding of activation in stimulated PMNs were assessed by FACS analysis of PMN surface markers and intracellular caspase-1 activity (data not shown), IL-1β secretion in supernatant, and overall cytotoxicity.

Pilot studies on the supernatants of MSU-stimulated blood PMNs suggest the potential of a dose-dependent, though minimal, IL-1β secretion. To corroborate these findings, experimental replications are required using a higher amount of isolated PMNs per well, and/or a more sensitive ELISA for IL-1β. Since IL-1β lacks a signal peptide necessary for conventional secretion, it is widely hypothesized that the cytokine must be released upon cell death[32]. While investigating this possibility, our data from the LDH cytotoxicity assay show that the dual PAMP +DAMP activation with LPS+ATP, leads to the greatest amount of cell death among stimulated PMNs. However, comparison of our stimulation methods with saponin-lysed and heat-killed PMNs (strong positive controls of cell death) show that the former did not promote cell death in the majority of PMNs, despite significant IL-1β release, suggesting that PMNs may release IL-1β while remaining alive. Stimulating macrophages/monocytes and assessing cytotoxicity accordingly will clarify the relative viability of PMNs and potentially, the disjunction between PMN death and IL-1β secretion.

Our combined approach using *ex vivo* analysis of human airway and blood samples, *in vitro* IL-1β bioactivity assays, and PMN stimulation assays corroborates a potential role of bioactive IL-1β in PMN-driven airway inflammation in CF. Follow-up studies confirming our results will pave the way for the development of effective immunomodulatory treatments to improve the quality of life of CF patients.

V. *Tables and Figures*

Gender	Visit Type	Age (y)	CFTR Mutation	FVC (l)	Azith	Tobra	*Staphylococcus aureus*	*P. aeruginosa*	*Candida albicans*	*Aspergillus fumigatus*
Female	O	24	HZ	2.28	No	Yes	No	No	No	No
Male	O	46	HZ	3.58	No	No	ND	ND	ND	ND
Female	O	23	HZ	2.29	Yes	No	S	M	Yes	Yes
Female	O	40	HZ	2.50	Yes	Yes	ND	ND	ND	ND
Female	I	31	HO	1.53	Yes	No	R	P	No	No
Female	I	24	HZ	2.94	Yes	Yes	R	No	Yes	No
Male	I	24	OT	2.98	No	Yes	No	M	No	No
Male	I	24	HZ	3.67	Yes	Yes	S	M	No	No
Female	I	24	HO	2.15	Yes	Yes	R	M	Yes	No
Male	O	24	HO	2.48	Yes	Yes	R	M	No	No
Male	O	31	HO	4.67	Yes	Yes	ND	ND	ND	ND
Male	I	19	HO	3.34	No	No	S	M	No	No
Male	O	25	HO	4.12	No	No	R	No	No	No
Male	I	31	HZ	4.49	Yes	Yes	No	P	Yes	Yes
Female	I	36	HZ	3.75	Yes	No	R	No	Yes	No
Female	I	23	HO	4.20	Yes	Yes	No	M	No	No
Female	O	25	HO	2.67	Yes	Yes	ND	ND	ND	ND
Female	O	24	HZ	3.09	Yes	Yes	R	P	No	No
Male	O	37	HZ	ND	No	Yes	R	M	No	No
Male	I	27	HO	2.56	Yes	Yes	No	M	No	No
Male	I	20	HO	3.25	No	Yes	S	M	No	No
Male	I	29	HO	ND	Yes	Yes	S	M	No	No
Female	I	31	HO	1.86	No	Yes	R	M	No	No
Female	I	29	HZ	1.41	Yes	No	No	M	No	No
Female = 12 Male = 12	O = 10 I = 14	28.0 ± 1.32	HO = 12 HZ = 11 OT = 1	2.99 ± 1.6	Yes = 16 No = 8	Yes = 17 No = 7	S = 5 R = 9 No = 6 ND = 4	P = 3 M = 13 No = 4 ND = 4	Yes = 5 No = 15 ND = 4	Yes = 2 No = 18 ND = 4

Infection status for *P. aeruginosa*: M, mucoid; P, planktonic.
Infection status for *S. aureus*: R, methicillin resistant; S, methicillin sensitive.
Azith, azithromycin; HO, δF508 homozygote; HZ, compound heterozygotes (comprising one δF508 and another mutation of the CF gene); I, inpatient visit; ND, not determined; O, outpatient visit; OT, two mutations other than δF508; Tobra, tobramycin.

Table 1: **Demographic data of CF patients** [27]

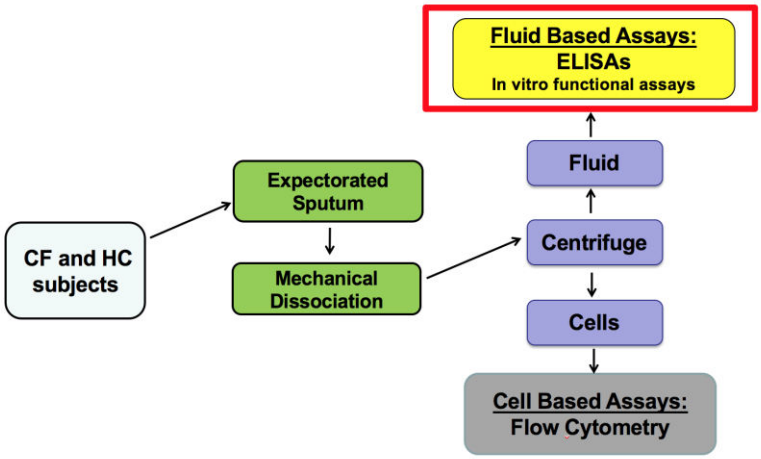

Figure 1: Diagram of ASN collection and processing

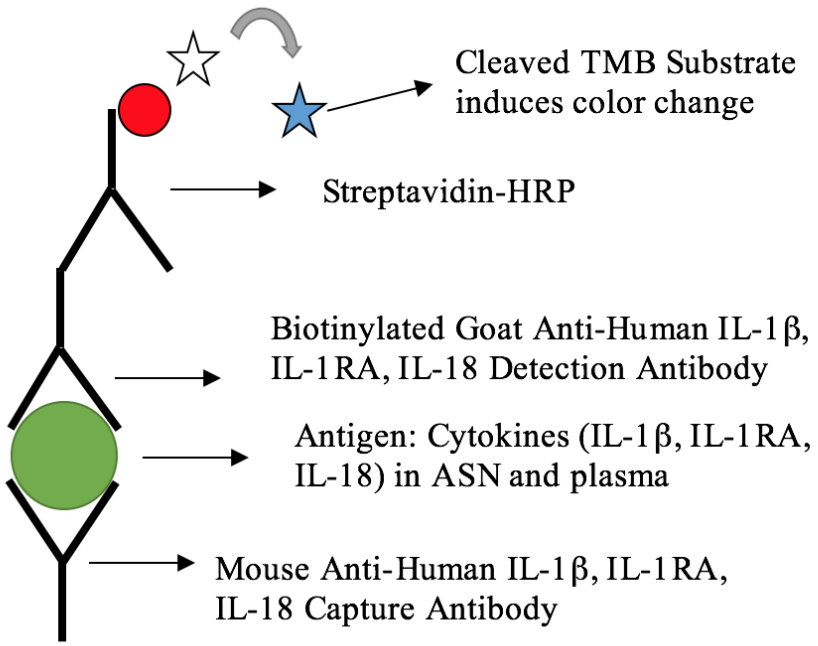

Figure 2: Schematic of a Sandwich ELISA used for cytokine quantification in CF and HC samples

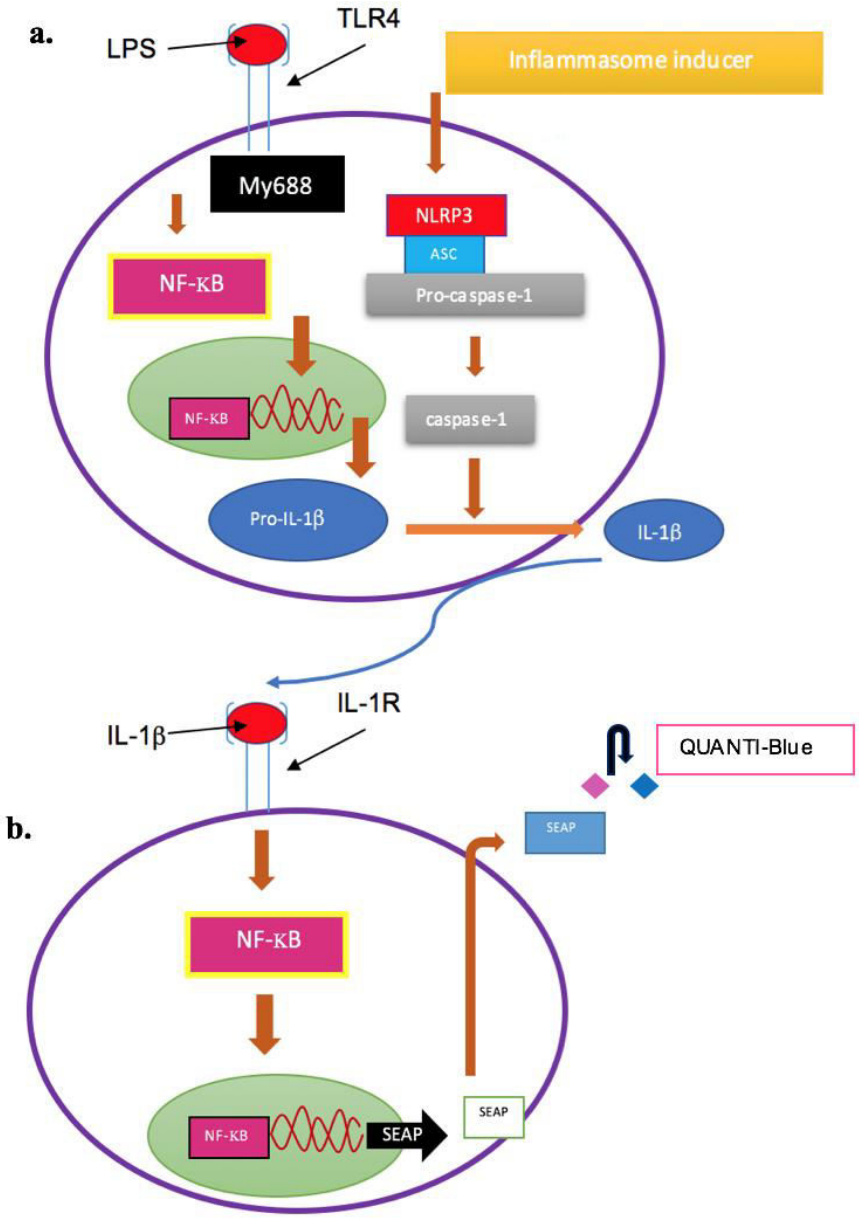

Figure 3: Principle of HEK-Blue assay. **a.** Priming THP-1 cells with LPS induces the production of pro-IL-1β via NF-κB activation. Subsequent stimulation with inflammasome inducers leads to downstream caspase-1 activation, which cleaves pro-IL-1β into the mature, secreted form. Note: Here, CF and HC samples with known IL-1β concentrations were used in lieu of the primed THP-1 cell line. **b.** IL-1β-containing samples are added to bioactive human IL-1β sensor cells. Binding of IL-1β to the IL-1 receptor leads to NF-κB activation and subsequent production of secreted embryonic alkaline phosphatase (SEAP). SEAP levels are quantified using the Quanti-Blue method, in which the intensity of color change from pink to blue reflects alkaline phosphatase activity.

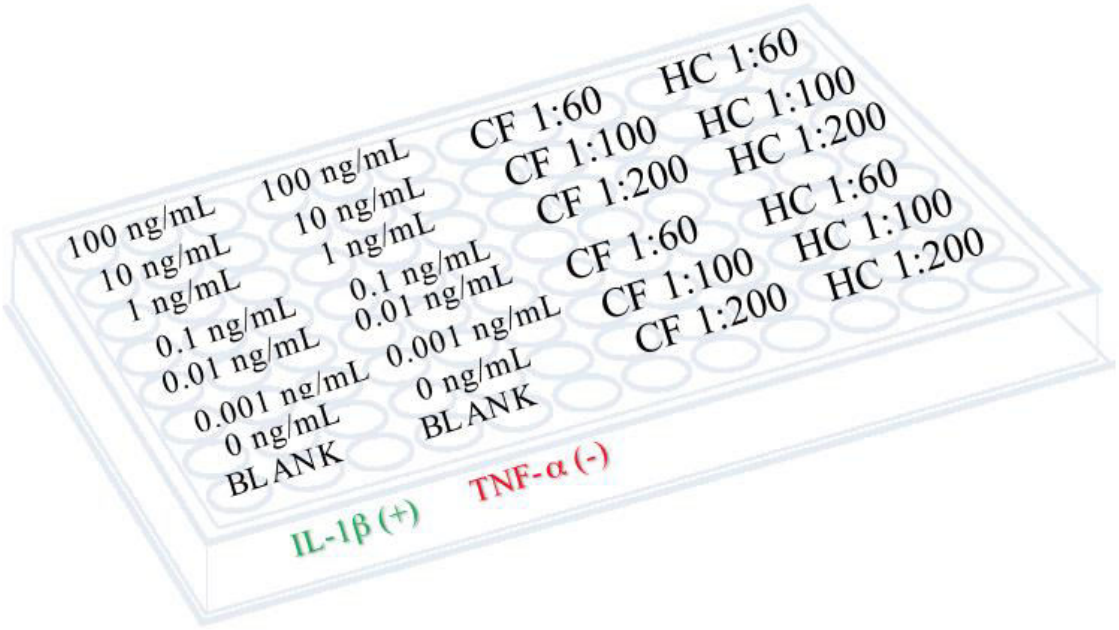

Figure 4: HEK-Blue Assay sample plate used to detect bioactive IL-1β in airway sputum

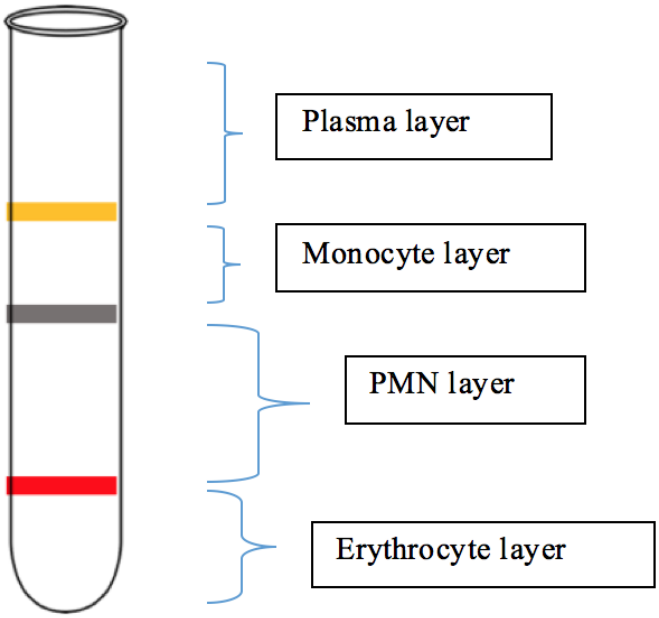

Figure 5: Diagram of blood layers following density centrifugation

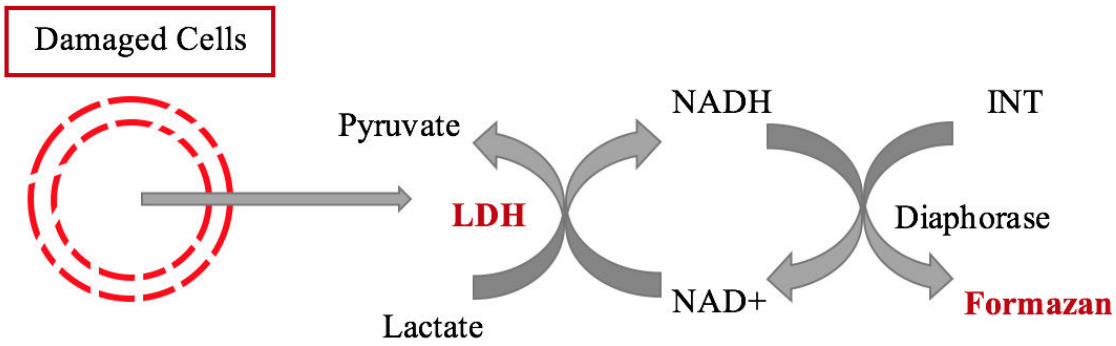

Figure 6: LDH cytotoxicity assay mechanism

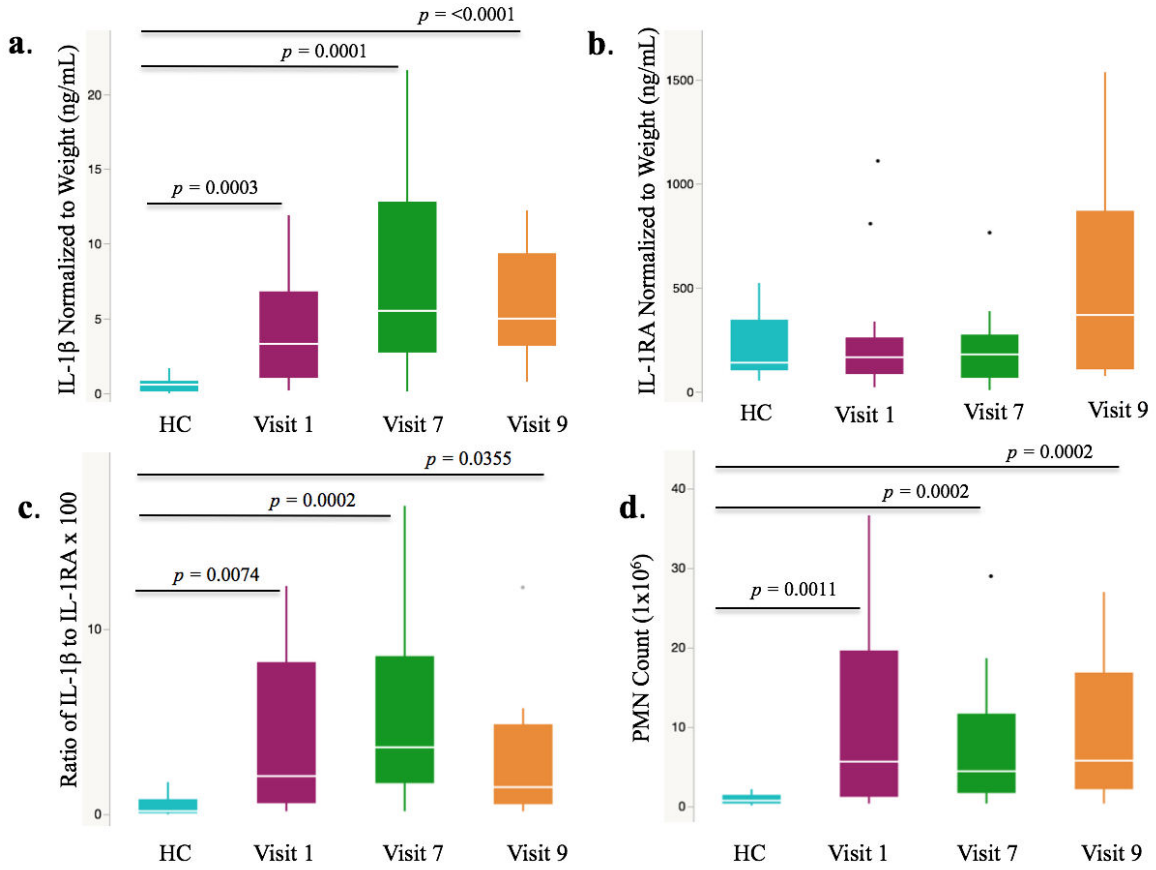

Figure 7: IL-1β and cell count is significantly up-regulated in CF ASN compared with HC ASN, whereas IL-1RA concentration is not significantly different across the board. (**a**) IL-1β was quantified via ELISA in airway samples from both HC (*n=9*) and CF (*n*=23, 22, 14 for visits 1, 7, and 9, respectively) subjects. A non-linear 4-parameter standard curve fit was used to calculate relative concentrations from optical density (O.D) values at 450nm minus blank O.D values. Duplicate sample concentrations (pg/mL) were then averaged, multiplied by the dilution factor used in assay preparation, and normalized to respective sputum weight. IL-1β concentration was reported in ng/mL. (**b**) IL-1RA was quantified via ELISA in airway samples from both HC (*n=9*) and CF (*n*=23, 22, 14 for visits 1, 7, and 9, respectively) subjects; data was processed in the same way. (**c**) Ratios were calculated according to values obtained for both cytokines. (**d**) PMN count in HC and CF sputum was determined by a hemocytometer. HC (*n=9*) and CF (*n*=23, 23, 14 for visits 1, 7, and 9, respectively). Significance was established by Mann-Whitney $U = 23.5$, 17, 3 (**a** from left to right) $U = 25$, 11, 16 (**b**) $U = 29.5$, 21, 9 (**c**) - p value < 0.05 two-tailed. p values over 0.05 not indicated.

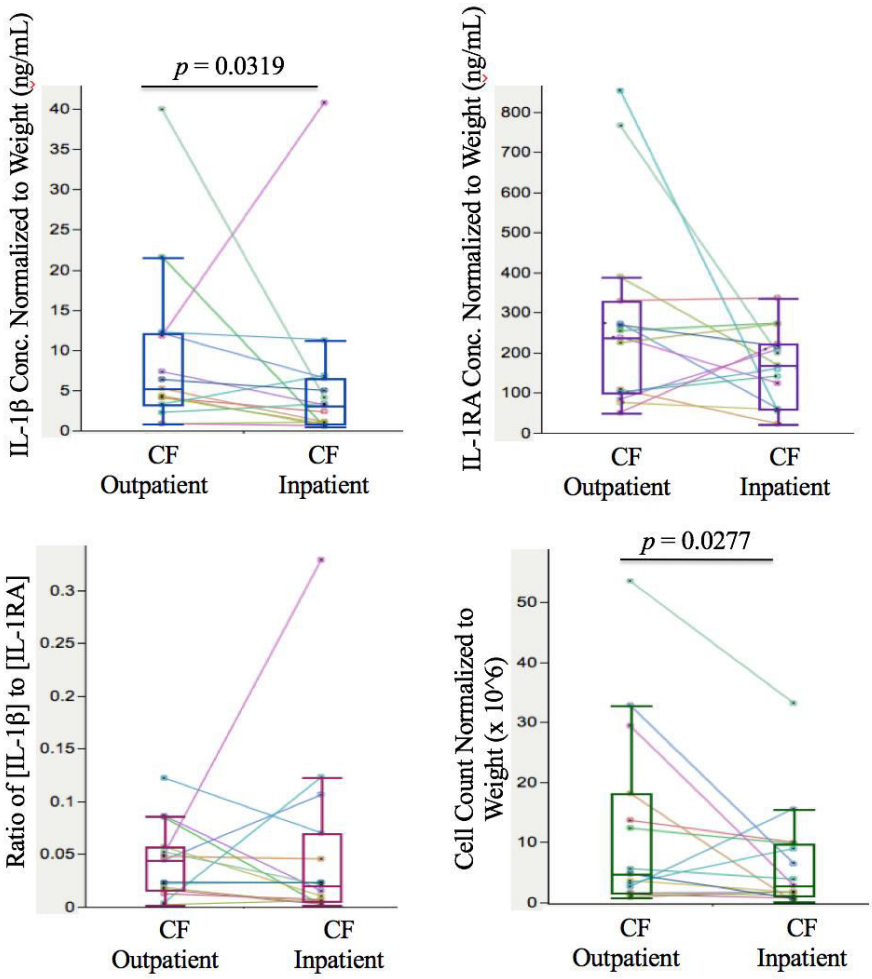

Figure 8: IL-1β and cell count are significantly lower during CF inpatient visits compared to CF outpatient visits, while IL-1RA quantity is not significantly different between visit types. The same data collection and processing protocol used in Figure 7 was followed to obtain these results. Outpatient and inpatient samples were matched by subject (n=15). Statistical analysis was done using the paired Wilcoxon signed-rank test. Significance was established with a two-tailed p value < 0.05. p values over 0.05 not indicated.

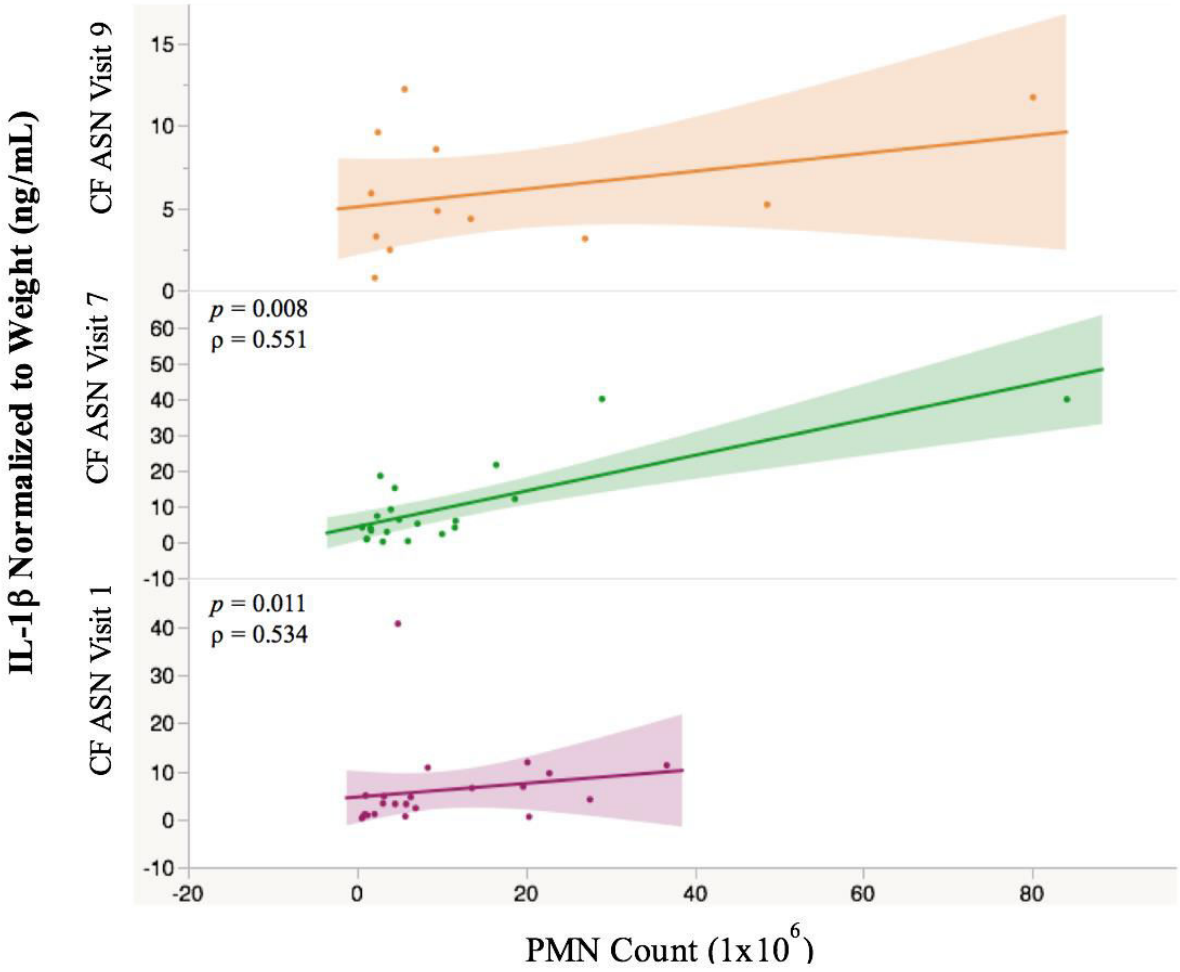

Figure 9: IL-1β is significantly correlated with PMN count in visit 1 and 7, but not in visit 9. Non-parametric correlation was done using the Spearman's test, with a 95% confidence region as shown. (n = 22, 21, 12 in visits 1, 7, and 9, respectively). Significance was established with a two-tailed p value < 0.05. p values over 0.05 not indicated. Spearman's rank correlation coefficient (ρ) reflected strong positive correlations between IL-1β concentration and PMN count.

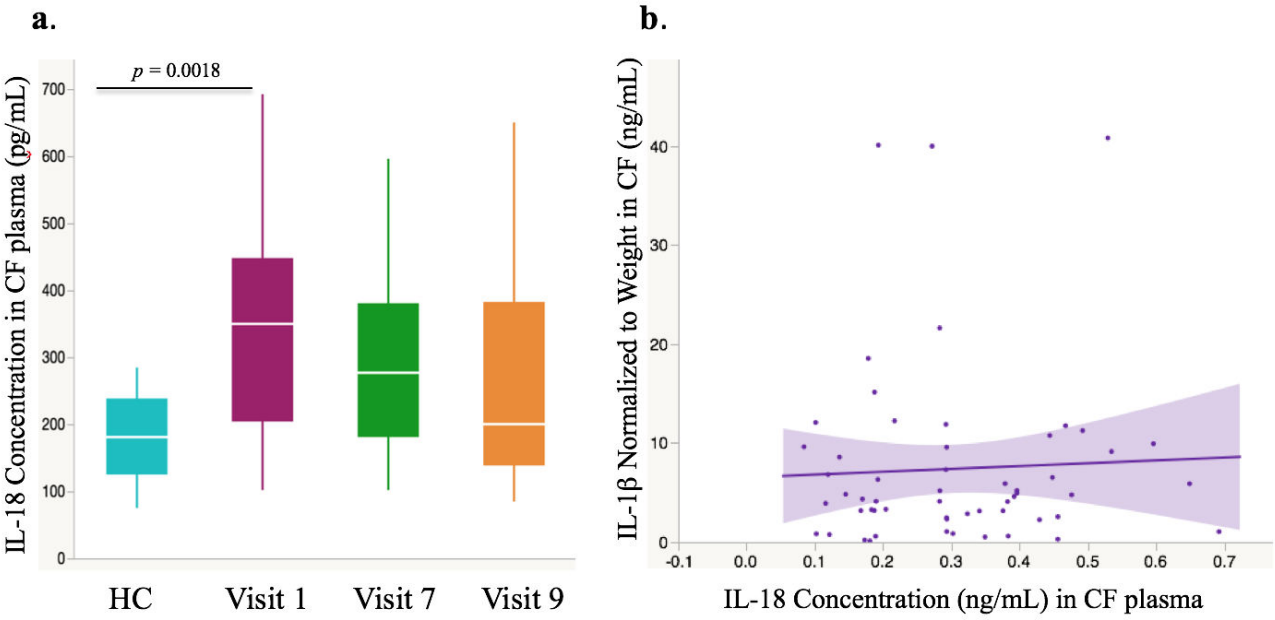

Figure 10: IL-18 concentration is significantly greater in CF Visit 1 plasma compared to HC plasma, but not between HC and the other CF visit types. (**a**) IL-18 was quantified using previously described ELISA methods and data analysis. Significance was established by Mann-Whitney $U = 32$ (**a**) - p value < 0.05 two-tailed. p values over 0.05 not indicated. CF Visit 1 plasma (n=23), CF Visit 7 plasma (n=22), CF Visit 9 plasma (n=14), HC plasma (n=9). (**b**) IL-1β in CF ASN is not correlated with IL-18 in corresponding CF plasma (Spearman test).

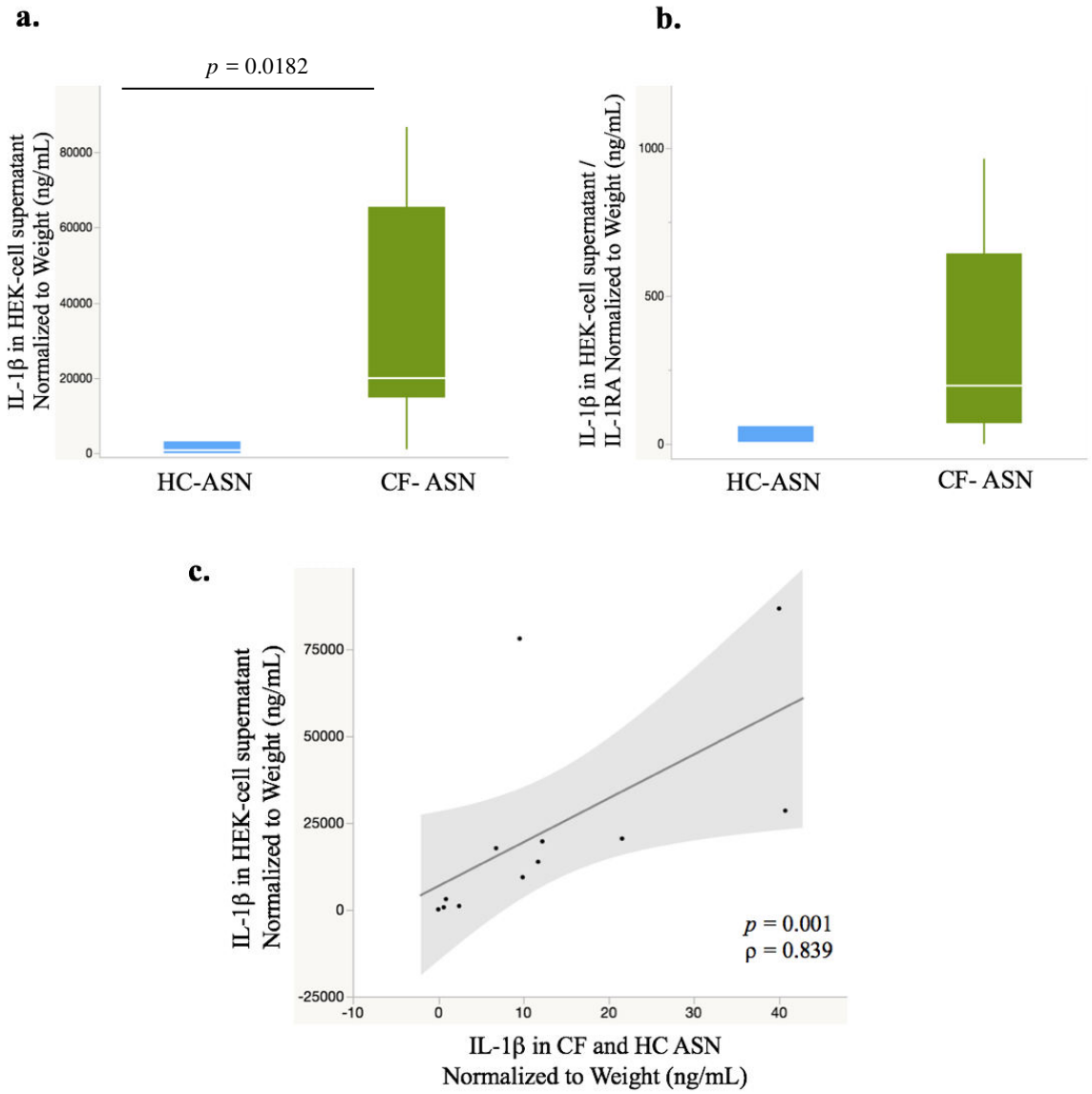

Figure 11: Bioactive IL-1β signaling is significantly up-regulated in HEK-Blue IL-1β cells when induced with CF-ASN compared to with HC-ASN. (**a**) IL-1β concentrations were calculated in ng/mL based on a standard curve of human recombinant IL-1β, using comparisons in SEAP detection at 655 nm. Concentration values from triplicate wells were averaged, multiplied by a dilution factor of 60, and then normalized to the weight of the CF or HC sample used to induce each particular well. Significance was calculated using the Mann-Whitney test. (**b**) Ratios were calculated of bioactive IL-1β normalized to weight (from Figure 11a) to respective normalized IL-1RA values (from Figure 7b). (**c**) Bioactive IL-1β SEAP readout (Y axis) induced by both CF and HC ASN samples is significantly correlated with matched *in vivo* IL-1β concentrations (X axis) in those samples (**from Figure 7a**). Significance was established by Mann-Whitney $U = 1$ (**a**) - p value < 0.05 two-tailed and a high ρ value from the Spearman test (n=12). p values over 0.05 not indicated.

a.

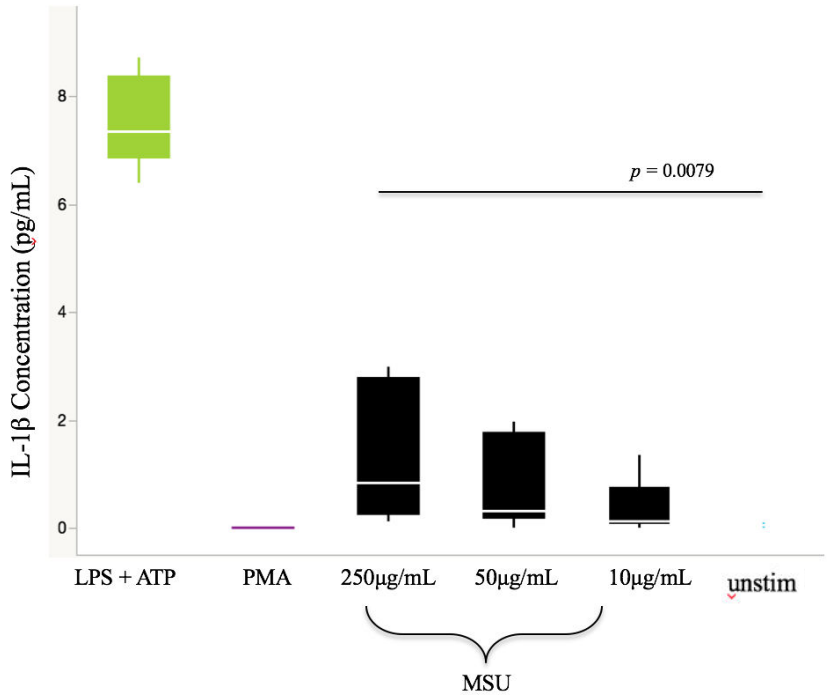
IL-1β Concentration (pg/mL)
8
6
4
2
0
p = 0.0079
LPS + ATP
PMA
250µg/mL
50µg/mL
10µg/mL
unstim
MSU

b.

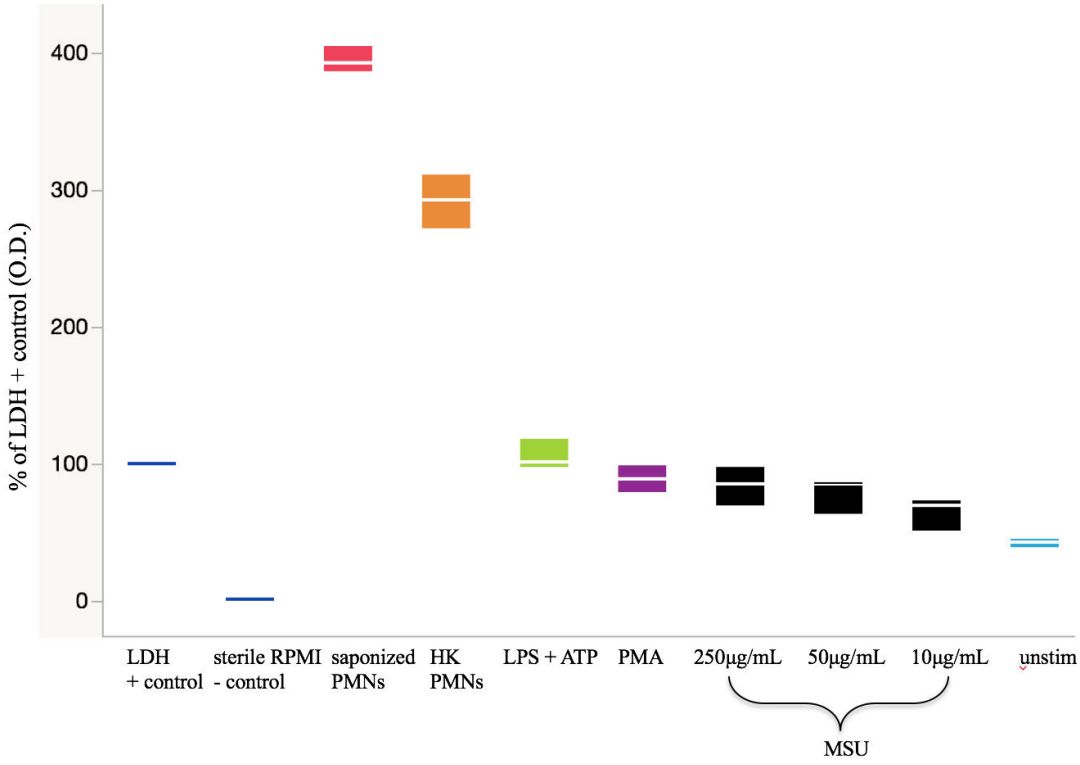
% of LDH + control (O.D.)
400
300
200
100
0
LDH + control
sterile RPMI - control
saponized PMNs
HK PMNs
LPS + ATP
PMA
250µg/mL
50µg/mL
10µg/mL
unstim
MSU

Figure 12: IL-1β production and secretion is up-regulated in stimulated PMNs compared with unstimulated PMNs and cell death is not induced in a dose-dependent manner. (a) Stimulated blood neutrophil supernatants from multiple inflammasome activation experiments (differing MSU concentrations, LPS (10ng/mL) + ATP (5mM), PMA (20nM) or unstimulated RPMI condition (n=5 for all 4 conditions)) were thawed from -80ºC, diluted 1:1 in reagent diluent, and plated in triplicate before undergoing subsequent standard ELISA analysis. Calculated IL-1β concentrations were averaged and doubled. p values were not significant enough between the MSU conditions to suggest a dose-dependent IL-1β secretion process, however the PMNs treated with 250μg/mL of MSU secreted drastically greater amounts of IL-1β than those unstimulated in solely RPMI (unstim). Significance was established by Mann-Whitney $U = 0$ (**a**) - p value < 0.05 two-tailed. p values over 0.05 not indicated. **(b)** The same thawed supernatants, in addition to those of saponized and heat-killed (HK) PMNs, were assayed for cytotoxicity. LDH activity was reported as % [(LDH at 490 nm) – (LDH at 680 nm)] optical density (O.D.) of 1xLDH Positive Control. *Monosodium urate (MSU), lipopolysaccharide (LPS), adenosine triphosphate (ATP), phorbol 12-myristate acetate (PMA)

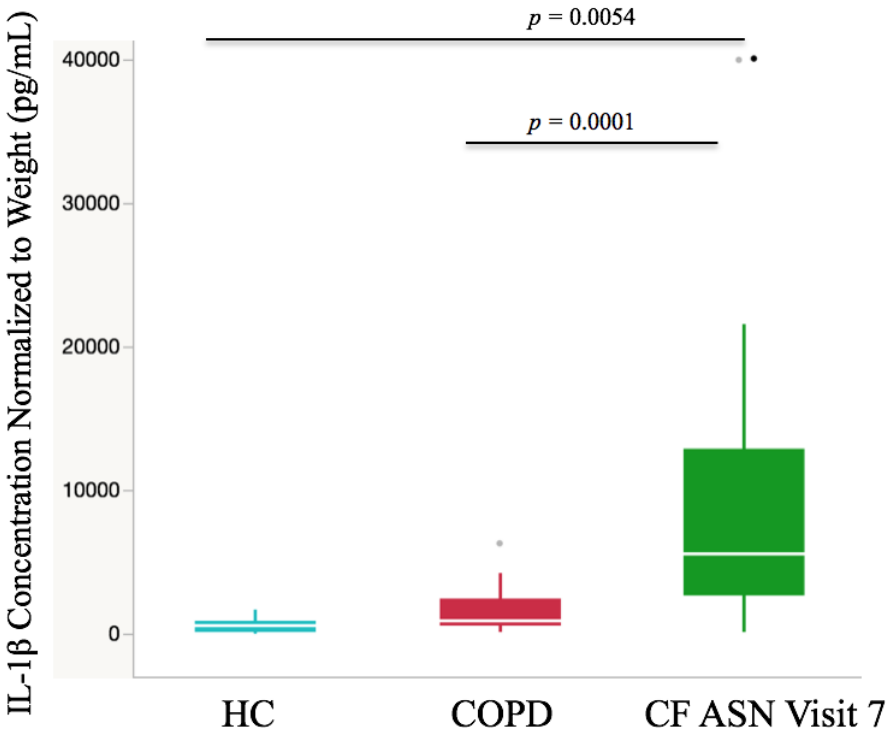

Figure 13: IL-1β concentration is significantly higher in CF visit 7, compared to HC and COPD patient samples. IL-1β concentration was quantified by ELISA in COPD patients (n = 10) as another PMN-dominated disease control. Concentrations of duplicated wells were averaged, multiplied by either 2 or 10, depending on the dilution factor used, and normalized to sputum weight. IL-1β concentrations in CF ASN from visit 7 patients and HC subjects were used as a comparison (n = 22 and 9, respectively). There was no significant difference between HC and COPD patient samples). Significance was established by Mann-Whitney U = 43, 17 - p value < 0.05 two-tailed. p values over 0.05 not indicated.

VI. References

1. Hayes, E., Pohl, K., McElvaney, N. G. & Reeves, E. P. The Cystic Fibrosis Neutrophil: A Specialized Yet Potentially Defective Cell. *Arch. Immunol. Ther. Exp. (Warsz.)* **59,** 97–112 (2011).
2. Rosenecker, J., Huth, S. & Rudolph, C. Gene therapy for cystic fibrosis lung disease: current status and future perspectives. *Curr. Opin. Mol. Ther.* **8,** 439–445 (2006).
3. MacKenzie, T. *et al.* Longevity of patients with cystic fibrosis in 2000 to 2010 and beyond: survival analysis of the Cystic Fibrosis Foundation patient registry. *Ann. Intern. Med.* **161,** 233–241 (2014).
4. Hwang, T.-C. & Kirk, K. L. The CFTR ion channel: gating, regulation, and anion permeation. *Cold Spring Harb. Perspect. Med.* **3,** a009498 (2013).
5. Okiyoneda, T. & Lukacs, G. L. Fixing cystic fibrosis by correcting CFTR domain assembly. *J. Cell Biol.* **199,** 199–204 (2012).
6. Mall, M. *et al.* The DeltaF508 mutation results in loss of CFTR function and mature protein in native human colon. *Gastroenterology* **126,** 32–41 (2004).
7. Boucher, R. C. New concepts of the pathogenesis of cystic fibrosis lung disease. *Eur. Respir. J.* **23,** 146–158 (2004).
8. Gibson, R. L., Burns, J. L. & Ramsey, B. W. Pathophysiology and Management of Pulmonary Infections in Cystic Fibrosis. *Am. J. Respir. Crit. Care Med.* **168,** 918–951 (2003).
9. Tirouvanziam, R., Khazaal, I. & Péault, B. Primary inflammation in human cystic fibrosis small airways. *Am. J. Physiol. - Lung Cell. Mol. Physiol.* **283,** L445–L451 (2002).

10. Rosenfeld, M., Ramsey, B. W. & Gibson, R. L. Pseudomonas acquisition in young patients with cystic fibrosis: pathophysiology, diagnosis, and management. *Curr. Opin. Pulm. Med.* **9,** 492–497 (2003).

11. Theilgaard-Mönch, K., Porse, B. T. & Borregaard, N. Systems biology of neutrophil differentiation and immune response. *Curr. Opin. Immunol.* **18,** 54–60 (2006).

12. Nakamura, H., Yoshimura, K., McElvaney, N. G. & Crystal, R. G. Neutrophil elastase in respiratory epithelial lining fluid of individuals with cystic fibrosis induces interleukin-8 gene expression in a human bronchial epithelial cell line. *J. Clin. Invest.* **89,** 1478–1484 (1992).

13. Kim, R., Pinkerton, J., Gibson, P., Cooper, M., Horvat, J. and Hansbro, P. Inflammasomes in COPD and neutrophilic asthma. *Thorax* 70: 1199-1201 (2015).

14. Baroja-Mazo, A. *et al.* The NLRP3 inflammasome is released as a particulate danger signal that amplifies the inflammatory response. *Nat. Immunol.* **15,** 738–748 (2014).

15. Nicholson, D. W. Caspase structure, proteolytic substrates, and function during apoptotic cell death. *Cell Death Differ.* **6,** 1028–1042 (1999).

16. Smith, D. E. The biological paths of IL-1 family members IL-18 and IL-33. *J. Leukoc. Biol.* **89,** 383–392 (2011).

17. Lee, J.-K. *et al.* Differences in signaling pathways by IL-1β and IL-18. *Proc. Natl. Acad. Sci. U. S. A.* **101,** 8815–8820 (2004).

18. Chan, E. D., Choi, H.-S., Cool, C., Accurso, F. J. & Fantuzzi, G. Interleukin-18 expression in cystic fibrosis lungs*. *Chest* **121,** 84S–85S (2002).

19. Bonar, S. L. *et al.* Constitutively Activated NLRP3 Inflammasome Causes Inflammation and Abnormal Skeletal Development in Mice. *PLOS ONE* **7,** e35979 (2012).

20. Cassel, S. L., Joly, S. & Sutterwala, F. S. The NLRP3 inflammasome: a sensor of immune danger signals. *Semin. Immunol.* **21,** 194–198 (2009).

21. Arun K Mankan, T. D. The NLRP3/ASC/Caspase-1 axis regulates IL-1beta processing in neutrophils. *Eur. J. Immunol.* **42,** 710–5 (2012).

22. Weber, A., Wasiliew, P. & Kracht, M. Interleukin-1 (IL-1) Pathway. *Sci Signal* **3,** cm1–cm1 (2010).

23. Abderrazak, A. *et al.* NLRP3 inflammasome: from a danger signal sensor to a regulatory node of oxidative stress and inflammatory diseases. *Redox Biol.* **4,** 296–307 (2015).

24. Dinarello, C. A., Simon, A. & van der Meer, J. W. M. Treating inflammation by blocking interleukin-1 in a broad spectrum of diseases. *Nat. Rev. Drug Discov.* **11,** 633–652 (2012).

25. Dinarello, C. A. Biologic basis for interleukin-1 in disease. *Blood* **87,** 2095–2147 (1996).

26. Normocin - Prevention Against Mycoplasma, Bacteria and Fungi as a routine addition to cell culture. Available at: http://www.invivogen.com/normocin.

27. Ingersoll, S. A. *et al.* Mature Cystic Fibrosis Airway Neutrophils Suppress T Cell Function: Evidence for a Role of Arginase 1 but Not Programmed Death-Ligand 1. *J. Immunol.* 1500312 (2015).

28. Eickmeier, O. *et al.* Sputum biomarker profiles in cystic fibrosis (CF) and chronic obstructive pulmonary disease (COPD) and association between pulmonary function. *Cytokine* **50,** 152–157 (2010).

29. Lappalainen, U., Whitsett, J. A., Wert, S. E., Tichelaar, J. W. & Bry, K. Interleukin-1beta causes pulmonary inflammation, emphysema, and airway remodeling in the adult murine lung. *Am. J. Respir. Cell Mol. Biol.* **32,** 311–318 (2005).

30. Hammad, D. R., Elgazzar, A. G., Essawy, T. S. & Abd El Sameie, S. A. Evaluation of serum interleukin-1 beta as an inflammatory marker in COPD patients. *Egypt. J. Chest Dis. Tuberc.* **64,** 347–352 (2015).

31. Reeves, E. P. *et al.* IL-8 dictates glycosaminoglycan binding and stability of IL-18 in cystic fibrosis. *J. Immunol. Baltim. Md 1950* **184,** 1642–1652 (2010).

32. Lopez-Castejon, G. & Brough, D. Understanding the mechanism of IL-1β secretion. *Cytokine Growth Factor Rev.* **22,** 189–195 (2011).